

**Accuracy of Sentinel-3 operational orbit predictions with increased solar activity**  
Mikel Catania<sup>(1)</sup>, Daniel Aguilar Taboada<sup>(2)</sup>, Daniel Martínez Díez<sup>(1)</sup>, Panagiotis Kremmydas<sup>(4)</sup>

<sup>(1)</sup>CLC Space GmbH at EUMETSAT  
Darmstadt, Germany

Email: [mikel.catania@external.eumetsat.int](mailto:mikel.catania@external.eumetsat.int), [daniel.martinezdiez@external.eumetsat.int](mailto:daniel.martinezdiez@external.eumetsat.int)

<sup>(2)</sup>EUMETSAT

Darmstadt, Germany

Email: [daniel.aguilartaboada@eumetsat.int](mailto:daniel.aguilartaboada@eumetsat.int)

<sup>(4)</sup>WGS Workgroup Solutions at EUMETSAT

Darmstadt, Germany

Email: [panagiotis.kremmydas@external.eumetsat.int](mailto:panagiotis.kremmydas@external.eumetsat.int)

**Abstract – The Sentinel-3 satellites fly around the Earth on a Sun-synchronous orbit with a repeat cycle of 27 days and cycle length of 385 orbits with the requirements to maintain ground-track deviation at all latitudes within  $\pm 1$  km of the reference ground track and the Mean Local Solar Time (MLST) deviation at the ascending nodes within  $\pm 90$  s from 22:00. Regular in-plane and out-of-plane manoeuvres are performed to maintain the orbit within requirements. Due to increased solar activity since mission start, the manoeuvres have become more frequent, and the planning and sizing of manoeuvres more challenging. This paper reviews the statistics of the accuracy of the orbit prediction, and how the increased solar activity has degraded these predictions. An analysis of observed decay rates and ground track deviation errors is presented, together with expected uncertainties. The paper discusses the approach and challenges of selecting acceptable drag scenarios for the optimization of operational manoeuvres.**

## I. INTRODUCTION

Sentinel-3 is a European Earth Observation satellite mission developed to support Copernicus ocean, land, atmospheric, emergency, security and cryospheric applications. It comprises two operational satellites, Sentinel-3A and Sentinel-3B, launched in 2016 and 2018 respectively, controlled in the current routine operational phase from the EUMETSAT facilities in Darmstadt, Germany.

Both satellites fly around the Earth on a Sun-synchronous orbit with a repeat cycle of 27 days and cycle length of 385 orbits, at an altitude of about 800 km. As per mission requirements, ground track deviation at all latitudes has to be kept within  $\pm 1$  km of the reference ground track and the MLST deviation at the ascending nodes within  $\pm 90$  seconds of 22:00. Both satellites share orbital plane and are separated by  $140^\circ$

in PSO.

The Sentinel-3 satellites are equipped with two sets of four 1 N monopropellant hydrazine thrusters to perform orbit maintenance manoeuvres.

The main perturbations at the Sentinel-3 orbit, apart from the non-spherical gravitational potential, are the atmospheric drag and the Sun and Moon interaction. The drag induces a semi-major axis decay, which is corrected by in-plane manoeuvres. The Sun and Moon perturbations induce a drift in inclination, which is corrected by out-of-plane manoeuvres.

## II. ORBIT CONTROL STRATEGY

The orbit control strategy was discussed in [1]. Different constraints drive the available size and position of manoeuvres, the main constraint being the need to perform out-of-plane manoeuvres within eclipse. The orbit control strategy comprises a regular schedule of three out-of-plane manoeuvres per year and a dynamic schedule of in-plane manoeuvres.

The out-of-plane manoeuvres are scheduled at fixed days of the year and make use of the whole eclipse interval to maximize the manoeuvre size and correct to the maximum extent possible the inclination. The result in ground track deviation is that at maximum latitudes the deviation approaches the  $+1$  km (Eastern) limit, and with the out-of-plane manoeuvre the ground track deviation is moved back close to the  $-1$  km (Western) limit. As will be seen in section VIII, this imposes a narrower band to the ground track deviation at the equator.

The in-plane manoeuvres are scheduled dynamically (although preferably scheduled on Wednesdays). The manoeuvres are sized such that the ground track deviation at all latitudes remains within requirements for as long as possible. If the orbit evolves as planned, only positive in-plane manoeuvres (which increase the semi-

major axis) are needed; in case the ground track deviation reaches the Western limit, a negative in-plane might be necessary, but the planning of in-plane manoeuvres tries to avoid this case.

The LTAN deviation is effectively controlled by the size and timing of the out-of-plane manoeuvres. Throughout the mission, the LTAN deviation has been kept within  $\pm 35$  seconds for both satellites, well within the requirements.

The partial history of ground track deviation and MLST deviation at descending node can be visualized in Fig. 1 and Fig. 2.

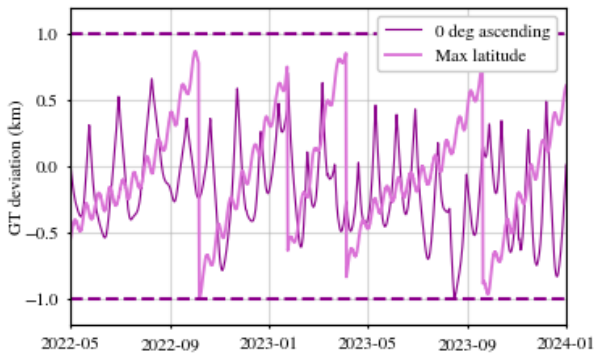


Fig. 1 – Ground track deviation of Sentinel-3B between 2022 and 2024. For simplicity, only the deviations at equator (ascending leg) and maximum latitude are shown. The out-of-plane manoeuvres create a visible jump in the deviation at maximum latitude. The effect of in-plane manoeuvres is evident in the deviation at the equator.

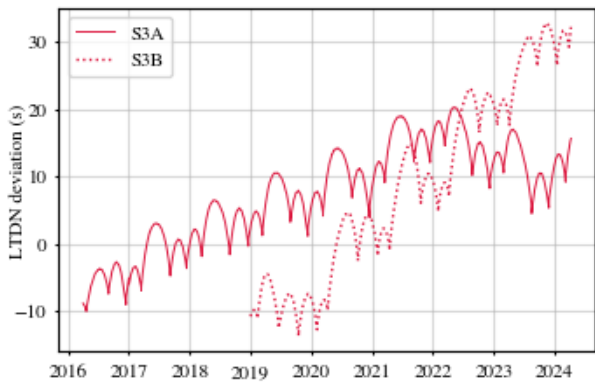


Fig. 2 – MLST deviation at descending node for both Sentinel-3A and Sentinel-3B. Each spike corresponds to an out-of-plane manoeuvre. The deviation is well within the  $\pm 90$  seconds requirement.

#### A. Impact of higher solar activity

The increase in solar activity has resulted in a higher atmospheric density, leading to an increased decay rate, which has been corrected with more frequent in-plane manoeuvres. The average interval between in-plane manoeuvres was more than two months in the years


2017 to 2020, and has decreased to between two and four weeks in 2023. Occasionally, the interval has been a week and even a few days when close to an out-of-plane manoeuvre.

Coupled with the increased decay rate and shorter in-plane manoeuvre interval, a bigger uncertainty in the orbital predictions has been observed, which has impacted negatively in the scheduling of manoeuvres. In the years 2022 and 2023 it has been necessary to replan manoeuvre dates with short notice in order to avoid a violation of the ground track deviation requirements. **Negative in-plane manoeuvres have also been needed, to avoid violations in the Western limit due to lower than expected solar activity.**

### III. OPERATIONAL SETUP

The expected evolution of the orbit is computed with a NAPEOS propagator. The setup includes a JGM3 gravity field model of degree and order 70, solid tides and other perturbations like the solar radiation pressure. For the atmospheric drag  $D$ , the model is based on the equation:

$$D = \frac{1}{2} \rho A C_D v^2, \quad (1)$$

where  $A$  is the frontal area,  $\rho$  the atmospheric density and  $v$  the speed of the spacecraft relative to the incident air. The atmospheric density is computed with the MSIS-90 model. Solar radio flux and geomagnetic activity indices are an input to the model. 

Note that the expected atmospheric drag, which is the main perturbing force and the less accurately modelled, is driven by the CD and solar activity predictions selected for a propagation; the following sections discuss the values considered for propagations and their accuracy.

**When sizing manoeuvres, in order to allow for uncertainties in the atmospheric drag model, higher-than-expected and lower-than-expected drag scenarios are considered. This is done by scaling the CD either up or down, resulting in an equivalent drag scale factor scenario. At the beginning of the mission a  $\pm 20\%$  margin was considered sufficient for these scenarios but, with increased solar activity, excursions from these scenarios became more frequent and it was evident that  $\pm 20\%$  was not enough. The drag scale factor is now changed to  $\pm 30\%$  since late 2023.**

### IV. ACCURACY OF SOLAR ACTIVITY PREDICTIONS

#### A. The solar cycle

Of the different indicators of solar activity (sunspot count, etc.), the Ap and F10.7 indices (together with the monthly average of the F10.7) are the ones used by the atmospheric density model. In the first years of the



mission (Sentinel-3A was launched in 2016 and Sentinel-3B in 2018) especially the F10.7 index remained relatively stable, with daily fluctuations that did not go above a small percentage of its value. With the onset of Solar Cycle 25, considered started in December 2019, there is an evident increase in solar activity, especially as registered by the F10.7 index, with values beginning a clear ramp-up in 2021. Not only the values are higher, but the day-to-day variance has also experienced a significant increase, with changes of 50% from one day to the next not uncommon. Fig. 3 shows the solar indices over the last few years.

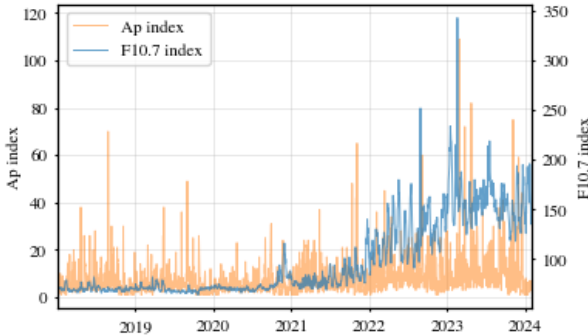


Fig. 3 – Daily values of the F10.7 and Ap indices. Since 2020 there has been an increase in solar activity, especially evident in the F10.7 index.

### B. Solar activity predictions

Each day, the solar activity of the following days is predicted with an ARIMA model that tries to catch the periodic oscillations of the solar indices. We can see how good these predictions have been by comparing them to the actual values later observed. Fig. 4 shows the errors of the F10.7 index at day  $n$  of prediction. The following two facts become apparent:

- Prediction errors increase with the day of prediction, but after about day 7 they remain more or less constant.
- Increase in solar activity has dramatically worsened the quality of the predictions.

Even on the day of prediction start itself the error can be over 10%, up to over 25% in subsequent days.

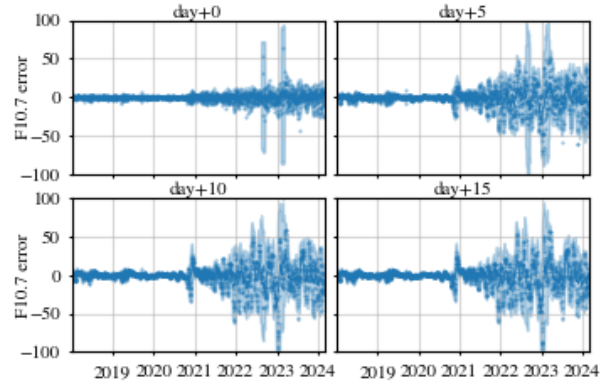


Fig. 4 – Error in predicted F10.7 index by day of prediction. The error is given in the same units as the F10.7 index.

For the Ap index the picture is more stable (see Fig. 5). There is no difference between the days of prediction, and the heteroscedasticity is also less apparent. This might be due to the high variability of the Ap index itself, where daily values can be an order of magnitude bigger than the average values.

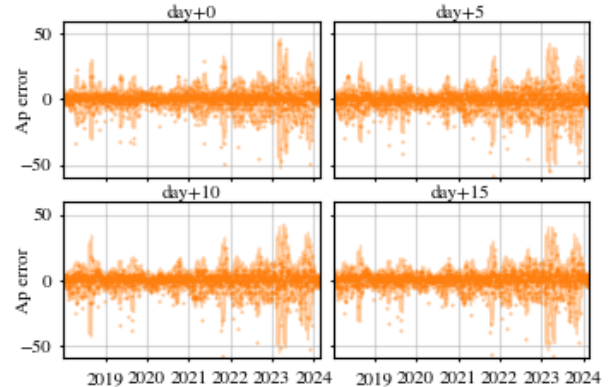


Fig. 5 – Error in predicted Ap index by day of prediction. The error is given in the same units as the Ap index.

## V. ACCURACY OF CD USED IN PROPAGATIONS

### A. Historical CD

The drag coefficient CD is used as a scaling factor in the atmospheric drag equation (1). The CD is a parameter estimated during the orbit determination process and in practice it absorbs the inaccuracies of the different models, most prominently the atmospheric drag model. During orbit determination, the value of the CD that best fits the observations (that come from onboard GNSS receivers) in an interval of 24 hours is estimated. This estimation has a fairly large variation, with estimated CDs ranging between 2 and 6 (on occasions over 8) throughout the mission, as seen in Fig. 6. Here, as with the solar indices discussed so far, the variability has increased in the period of increased solar activity.

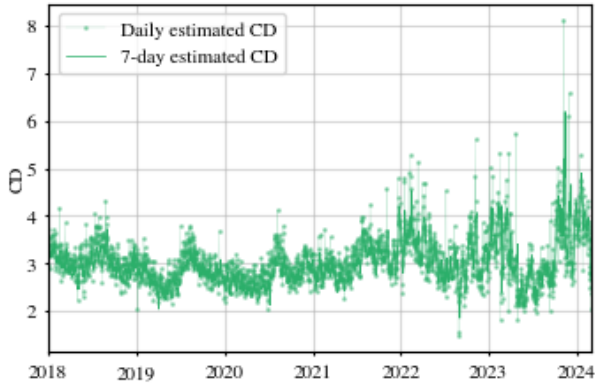


Fig. 6 – Sentinel-3A estimated CD. The dots represent the CD estimated in a 24-hour arc, while the continuous line is the estimation over a 7-day arc. The values for Sentinel-3B are similar.

### B. CD used in propagations

There is a wide range of options on the CD that can be used to propagate the orbit. At EUMETSAT we use a constant value: the CD that best fits into an orbit determination of the last 7 days. In practical terms this is very similar to the average of the CDs of the last 7 days. This curve is also shown in Fig. 6.

Fig. 7 shows the comparison between the CD used for propagations and the estimated CD as discussed in the previous paragraphs. The comparison shows the average error of the CD used in propagations compared to the estimated CD over two weeks following the day of propagation start. Again, the increased solar activity has led to worsened predictions. Whereas the error was around 10 to 20% before 2021, it was up to 60% in 2023. Even though there is no systematic bias, there is a periodic oscillation in the average error.

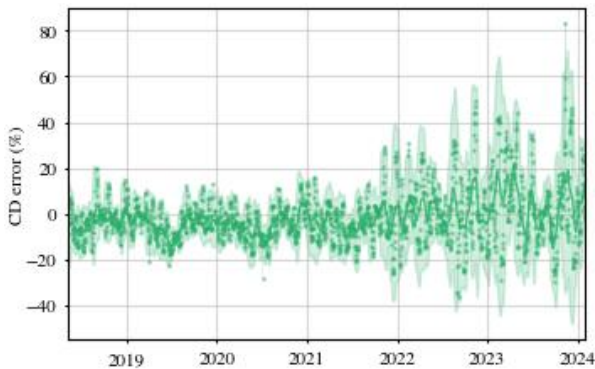


Fig. 7 – Error in the CD used for propagations in Sentinel-3A. The CD used at each propagation is compared to the later estimated CDs over a period of two weeks, and the comparison shows the average error. The values for Sentinel-3B are similar.

## VI. DECAY RATE STATISTICS

The evolution of the ground track deviation at the equator is driven by the semi-major axis decay and

associated orbital period reduction, which in turn is mainly driven by the atmospheric drag. SMA decay has a linear relationship with drag in the simplified potential model:

$$\frac{da}{dt} = 2 \sqrt{\frac{a^3 D}{\mu m}}$$

Here,  $a$  is the semi-major axis,  $m$  is the spacecraft mass, and  $\mu$  is the Earth's gravitational constant. Knowing the decay rate of both the propagated and the actual orbit, we can directly compare the drag of the propagation model to the real one, without needing to look into intermediate proxies like the density, and getting thus a direct evaluation of the model in regards to atmospheric drag.

The historical decay rate has been computed using a simplified computation from [2], using only the J2-corrected terms of the keplerian elements. An average over 57 orbits was done, which takes advantage of the sub cycle of the Sentinel-3 reference ground track.

Fig. 8 show this decay rate. Starting with a decay rate of about -0.3 m/day in the first years of the mission, the decay rate has increased to over -1 m/day in 2022, to even -4 m/day in some periods of 2023. Both Sentinel-3A and Sentinel-3B have experienced the same decay rate, which is expected since they fly at the same orbital plane with a phase difference of 140 deg, have the same aerodynamics characteristics and their mass is within 0.4% of each other.

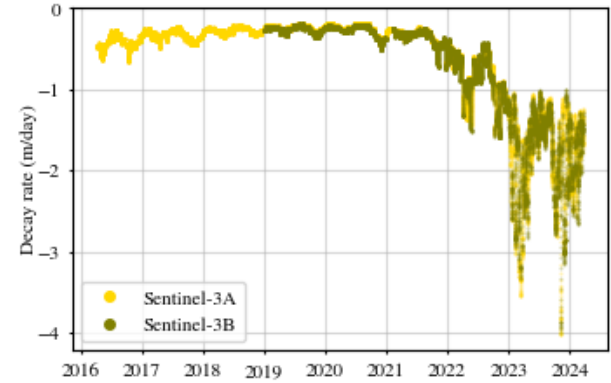


Fig. 8 – Sentinel-3A and Sentinel-3B observed decay rate. Six-monthly oscillations are apparent in the low solar activity period. With the solar activity increase, both the decay rate and its variance have increased.

It is interesting to see how the decay rate relates to the solar activity indices. Fig. 9 shows a 30-days moving average of the Sentinel-3A decay rate, the F10.7 and Ap indices, and the estimated CD. Clearly the decay rate follows the solar activity. Three periods are highlighted in 2023: at the beginning, there was a period of high decay rate and high F10.7 and Ap values. In the second period, even though the F10.7 index remained high, the decay rate was relatively lower, which could be explained by a lower geomagnetic activity shown by the

Ap index. In the atmospheric density model, this lower decay rate in a period of high solar activity is clearly compensated by estimating a lower CD. In the third period, again with high decay rate, the model compensates the relatively lower F10.7 index by estimating a higher CD.

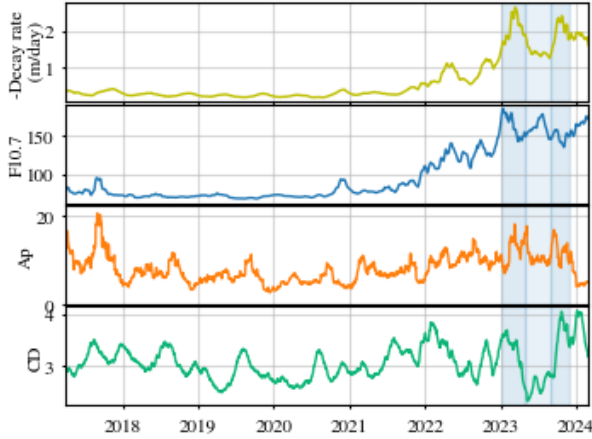


Fig. 9 – Running averages (30-day window) of the observed decay rate, solar indices, and CD for Sentinel-3A. Three periods of relatively high, low, and high decay rate in 2023 are highlighted, for a comparison with the solar activity and the estimated CD.

#### A. Decay rate of propagations

Propagations with the historical solar activity and CD values have been redone, covering several years of the mission. The propagations start at midnight of every day and are three weeks long. For each propagation, the average decay rate is computed, and compared to the average decay rate of the actual orbit (based on daily orbit determinations done at the time and validated against the precise orbit determination service) over the same period. The information of the actual orbit contains gaps, because the periods close to manoeuvres have to be discarded; for a valid comparison, only periods where the historical decay rate contains more than 50% information are considered. The result can be seen in Fig. 10. The error oscillated within 20% until 2022, and has increased to 60% in the next years.

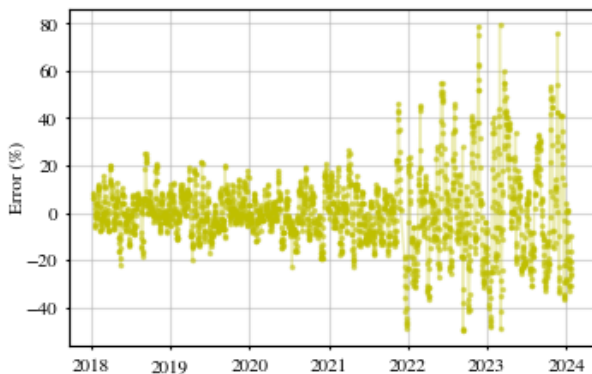


Fig. 10 – Error on average decay rate (equivalent to error on

atmospheric drag) of historical propagations compared to observed decay rate of Sentinel-3A.

The comparison could be used to show whether the drag scaling that is used in the extreme scenarios is correct. However, the same average decay can have very different effects in the ground track evolution, depending on how the decay is distributed (for example, a higher decay at the beginning of the period leads to a higher ground track deviation than if the higher decay was towards the end of the period due to its accumulated effect). Thus, to have a better idea of the margins that should be used in operations, one has to follow the inverse approach: take a look at the statistics of ground track deviation errors and infer what is the drag scale factor that leads to the same ground track deviation error.

## VII. GROUND TRACK DEVIATION ERROR STATISTICS

The propagations done to compute the decay rate have also been directly compared to the actual orbit. For each propagation, we get the along-track difference with respect to the actual orbit at different times. The along-track difference can be translated to ground track deviation difference at equator with the ratio of Earth's rotational speed to orbital speed:

$$\Delta GT = \frac{v_{EQ}}{v_{orb}} \Delta AT.$$

This ignores the small drift on LTAN over a propagation, which is negligible.

The comparison can only be done up to the next operational manoeuvre: after that, the actual orbit contains the effect of a manoeuvre that would make the comparison spurious. Due to the more frequent manoeuvres in 2022 and 2023, there are less intervals that cover the three weeks of propagation in those years.

The effect of the inaccuracies in the propagations result in ground track deviation differences with respect to the actual orbit that grow quadratically, as evidenced in Fig. 11. As explained before, some curves finish before the three weeks period because of manoeuvres. The heteroscedasticity is however very strong, and we cannot extract statistics that are valid for the whole mission. In Fig. 12 the same differences are plotted by day of propagation start, evidencing the worsening with the increased solar activity.

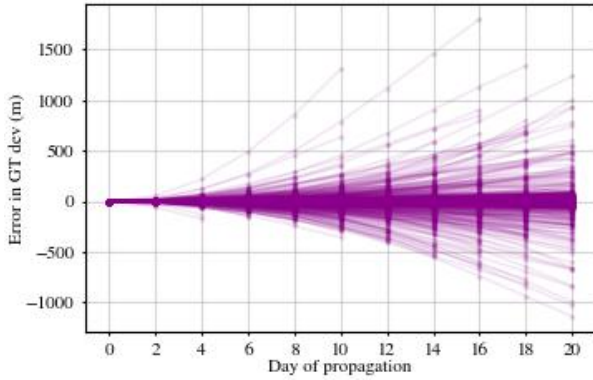


Fig. 11 – Difference in ground track deviation at equator of historical propagations of Sentinel-3A with respect to the actual orbit. The propagations are three weeks long, and there is a propagation per day between 2018 and 2024. The comparison can only be done up to the next manoeuvre.

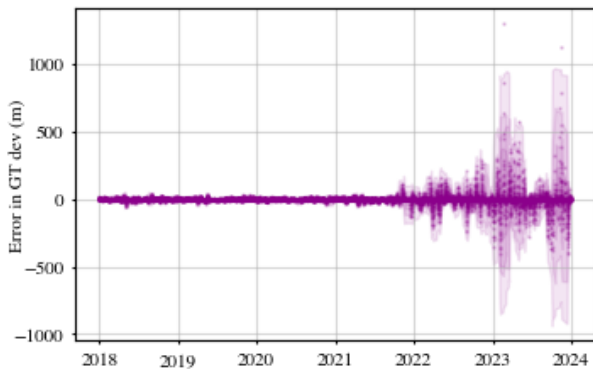


Fig. 12 – Difference in ground track deviation at equator of historical propagations of Sentinel-3A with respect to the actual orbit. The plot shows the same information as Fig. 11, but each propagation start is ordered in the x-axis, and the differences grow in the vertical axis.

The only choice is to get statistics by looking at selected intervals. Here, the statistics have been divided by years. The plot in Fig. 13 shows one standard deviation of the error in ground track deviation at each year of the mission. Although not shown, the distribution of errors resembles approximately a normal distribution. For 2023, due to the fewer long propagations because of more frequent manoeuvres, the parabolic shape is somewhat lost.

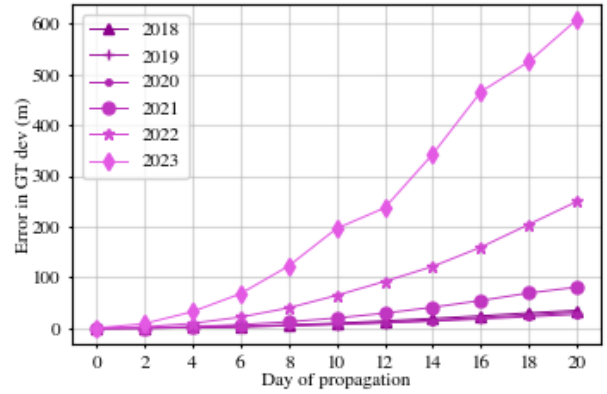


Fig. 13 – One standard deviation of the ground track deviation error of Sentinel-3A. The statistics are collected across a year. Due to fewer long propagations in 2023 because of more frequent manoeuvres, the shape is not as regular as in other years.

The statistics allow us to have knowledge of the expected ground track deviation error at day  $n$  of a propagation. Depending on the needs, we could use different margins: three standard deviations if we want to catch all cases, two standard deviations if we allow for the occasional excursion, or any other value that might be operationally meaningful.

#### A. Conversion into drag scale factor

Choosing a drag scale factor results in a ground track deviation difference with respect to the baseline scenario. With the same drag scale factor, the resulting ground track deviation difference depends on the underlying decay rate that the spacecraft is experiencing. We can use the decay rate experienced in the different years of the mission and see, with a given drag scale factor, how many standard deviations of the ground track deviation error it covers. This is shown in Fig. 14. The operational setup was a scaling factor of  $\pm 20\%$  until 2023. In the years of low solar activity this covered more than two standard deviations, but by 2022 this was closer to one standard deviation. This was evident by the fact that more negative in-plane manoeuvres were needed and more frequent rescheduling of manoeuvres, and the drag scale factor was increased to  $\pm 30\%$  in 2023. This covered two standard deviations again, which has resulted in a more robust operational setup, in exchange of more frequent in-plane manoeuvres.

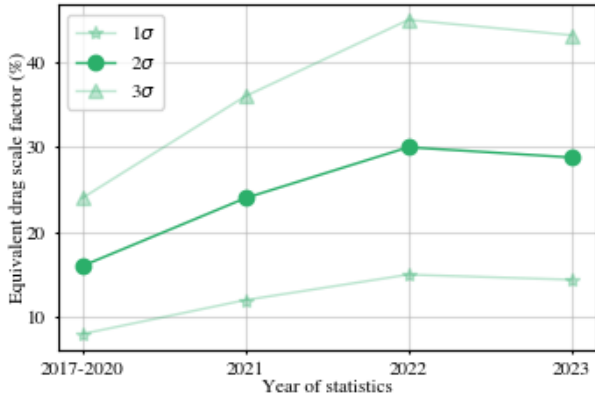


Fig. 14 – Selecting a drag scale factor results in a ground track deviation over the baseline scenario. This depends on the decay rate of the baseline scenario. The plot shows, for several years, how many standard deviations of ground track deviation error a given drag scale factor would be equivalent to.

## VIII. CONCLUSIONS

### A. Drag scale factors

The resulting statistics have confirmed that the decision to increase the drag scale factor margins from  $\pm 20\%$  to  $\pm 30\%$  was necessary with the increased solar activity. For the moment, the current value of  $\pm 30\%$  will continue covering most cases, but it does not exclude the need for the occasional negative in-plane manoeuvre. This is however desirable over increasing the drag scale factor, which would effectively increase the frequency of in-plane manoeuvres and overall operational workload.

The situation will continue to be monitored, and if repeating the statistics with increased solar activity shows that the current setup covers less cases, the operational margins might be adjusted.

### B. Out-of-plane manoeuvres

The main discussion has dealt with ground track deviations at equator, but the requirement is to control the ground track deviation at all latitudes. The evolution at maximum latitude is dictated by Sun and Moon perturbations more than by air drag, and in intermediate latitudes the deviation is approximately:

$$\Delta GT_{\text{PSO}} = \Delta GT_{\text{EQ}} \cos(\text{PSO}) + \Delta GT_{\text{max lat}} \sin(\text{PSO})$$

This ignores eccentricity, inducing an error especially in the southern hemisphere, but for this discussion it is a valid approximation.

The strategy of out-of-plane manoeuvres is to perform three manoeuvres per year, as outlined in [1]. This results in a ground track deviation at maximum latitudes that is close to the limits, see for example Fig. 15. In order to guarantee that the ground track deviation is

within limits at all latitudes, the deviation at the equator must now be controlled in a much narrower band.

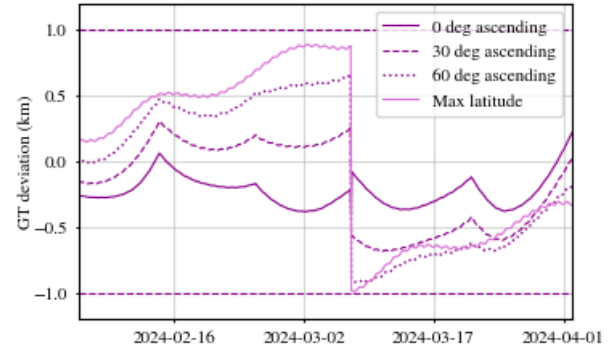


Fig. 15 – Ground track deviations at different latitudes (equator, 30 deg ascending, 60 deg ascending and maximum latitude) in a period centered around an out-of-plane manoeuvre. The deviation at maximum latitude is close to the limits, which forces the deviation at the equator to be inside a narrower band.

Since the ground track deviation errors have increased in the last years, keeping a narrow band translates into a very short manoeuvre cycle when close to out-of-plane manoeuvres. Indeed, with the discussed 30% drag scale factors the manoeuvre cycle in these periods is currently one week, and in some case it has been necessary to perform an in-plane just two days after an out-of-plane to avoid an excursion at intermediate latitudes.

One option is to reduce the size of the out-of-plane manoeuvres and keep the ground track deviation at maximum latitude in a narrower band, allowing for longer manoeuvre cycles. This would require more out-of-plane manoeuvres per year, resulting in a loss in efficiency as described in [1]. It can be operationally beneficial however, and probably necessary if the drag scale factors are further increased.

### C. Fixed manoeuvre cycles

The statistics shown in section VII allow for the definition of expected ground track deviation error at equator, depending on the day of propagation and the overall solar activity situation (low activity versus high activity). These values can be used to define the maximum duration between in-plane manoeuvres that guarantees that the ground track deviation will be kept within limits, which will depend on the solar activity. This could allow fixing manoeuvre slots (e.g. weekly or bi-weekly). There are operational aspects that would need to be considered, like holidays, CAMs, or allowance for unforeseen negative in-plane manoeuvres, but could also introduce a regularity that could be exploited for easier automation of operations.

This would be in contrast with the current operational approach, where each in-plane manoeuvre tries to

maximize the time until the next manoeuvre. For the moment, a switch in the approach is not considered, but is a potential change that could be backed up by the statistics shown.

#### IX. REFERENCES

- [1] D. Aguilar Taboada, J. M. de Juana Gamio and P. L. Righetti, "Sentinel-3 orbit control strategy", *27<sup>th</sup> ISSFD*, Melbourne, Australia, February 2019.
- [2] S. Spiridonova, M. Kirschner and U. Hugentobler, "Precise Mean Orbital Elements Determination for LEO Monitoring and Maintenance", *24<sup>th</sup> ISSFD*, Laurel, Maryland, USA, May 2014.